ETH
Eidgenössische Technische Hochschule Zürich
Swiss Federal Institute of Technology Zurich

Seminar for Applied Mathematics SAM

Hagedorn Wavepackets and Schrödinger Equation with Time-Dependent, Homogeneous Magnetic Field

V. Gradinaru and O. Rietmann

Research Report No. 2020-68
November 2020

Seminar für Angewandte Mathematik
Eidgenössische Technische Hochschule
CH-8092 Zürich
Switzerland

Hagedorn Wavepackets and Schrödinger Equation with Time-Dependent, Homogeneous Magnetic Field

Vasile Gradinaru, Oliver Rietmann

November 17, 2020

Abstract

Certain generalized coherent states, so-called Hagedorn wavepackets, have been used to numerically solve the standard Schrödinger equation. We generalize this approach and its recent enhancements to the magnetic Schrödinger equation for a time-dependent, spatially homogeneous magnetic field. In numerical experiments we examine the order of convergence and the preservation of norm and energy. We use this method to simulate a penning trap as proposed in recent work on quantum computing.

1 Introduction

The generalized coherent states introduced in [8], nowadays known as Hagedorn wavepackets, have been used successfully to design numerical methods for the Schrödinger equation [4]. The present work adapts the Hagedorn wavepacket approach to the Schrödinger equation for a (possibly time dependent) homogeneous magnetic field.
In [6] the authors generalize the well-known Fourier grid approach to the same equation. Using Hagedorn wavepackets we overcome several drawbacks of this Fourier approach: When charged particles are subject to a magnetic field, they start to spin in circles. These rotations can not be expressed exactly on the Fourier grid. Unlike the (discrete) Fourier basis functions, rotated Hagedorn wavepackets are again Hagedorn wavepackets. The time-propagation under the new magnetic field terms can thus be expressed exactly. In general, the Fourier grid approach is complementary to the Hagedorn approach in the following sense: The Fourier method is satisfactory for large values of the model parameter ε, while the Hagedorn approach improves for small values [4] (here, ε^2 plays the role of reduced Planck constant $\hbar$). Moreover, at least for localized (in space and momentum) solutions, the Hagedorn approach is more efficient in high dimensions [4].
First, we extend the so-called semiclassical splitting [5] to the non-zero magnetic field case. Recently, this approach has been further improved (for the zero magnetic field case) in [2] by the use of perturbation-aware splittings and of a modified potential. The key observation in generalizing these splitting schemes in a simple and efficient way is the following: The new terms due to the homogeneous magnetic field are infinitesimal rotations and commute with the rotation invariant Laplace operator. This allows us to decouple the associated time evolutions. We refer to [6, Sec. 2.1] for a more detailed explanation. In our simulations we observe the same convergence properties and need only minor additional effort to treat the new terms in presence of a magnetic field. More precisely, we only require the solution of an additional, low dimensional ODE.

Hagedorn wavepackets have been used for instance in [12] to solve the Schrödinger equation for non-homogeneous magnetic fields. The authors thereof mention the semiclassical splitting, but do not aim to generalize it to the magnetic Schrödinger equation. Our work thus differs in the sense that we consider only homogeneous (but time dependent) magnetic fields and we provide much more efficient methods. In fact, this seems to be the natural way to generalize the semiclassical splitting and its enhancements.
Homogeneous magnetic fields are used for instance in Penning traps to implement qubits in experimental quantum computing. We conduct our numerical experiments in this setting and use (a version of) the Hamiltonian proposed in [9].

2 The Magnetic Schrödinger Equation

Consider an electric potential $\phi(x,t)$ and a magnetic potential $A(x,t)$, where $x \in \mathbb{R}^d$ and A maps to $\mathbb{R}^d$. We assume that $d \geq 2$. For a particle of unit mass and unit charge, the Hamiltonian reads

$$\begin{aligned} H^\varepsilon &= \tfrac{1}{2}\left(-i\varepsilon^2\nabla - A\right)^2 + \phi \\ &= \tfrac{1}{2}\left(-\varepsilon^4\Delta + 2i\varepsilon^2 A\cdot\nabla + i\varepsilon^2(\nabla\cdot A) + \|A\|_{\mathbb{R}^d}^2\right) + \phi. \end{aligned}$$

The model parameter $\varepsilon^2 > 0$ plays the role of the reduced Planck constant. Now we consider the special case of an homogeneous magnetic field. It is convenient to describe the magnetic potential by a 1-form $A(x,t) = A_l(x,t)\,\mathrm{d}x^l$. The magnetic field being homogeneous then means that the magnetic field 2-form $\mathrm{d}A$ is independent of x. Therefore we choose

$$A(x,t) := B_{jl}(t)\, x^j \mathrm{d}x^l$$

where $B(t) = (B_{jl}(t))_{1\leqslant j,l\leqslant d}$ is a real, skew-symmetric matrix. The corresponding magnetic field 2-form is given by

$$\mathrm{d}A(t) = 2\sum_{1\leqslant j<l\leqslant d} B_{jl}(t)\ \mathrm{d}x^j\wedge\mathrm{d}x^l.$$

We introduce for $j,l\in\{1,\ldots,d\}$ the operators

$$\begin{aligned} p_l^\varepsilon &:= -i\varepsilon^2\partial_l && \text{(components of linear momentum)} \\ L_{jl}^\varepsilon &:= x_j p_l^\varepsilon - x_l p_j^\varepsilon && \text{(generalized angular momentum)} \end{aligned}$$

and

$$H_B^\varepsilon(t) := -\sum_{1\leqslant j<l\leqslant d} B_{jl}(t)\, L_{jl}^\varepsilon. \tag{2.1}$$

For this particular vector potential, we have

$$i\varepsilon^2 A\cdot\nabla = H_B^\varepsilon(t), \quad (\nabla\cdot A)\equiv 0, \quad \tfrac{1}{2}\|A\|_{\mathbb{R}^d}^2 = \tfrac{1}{2}\|B(t)\,x\|_{\mathbb{R}^d}^2$$

and our Hamiltonian thus reads

$$H^\varepsilon = \underbrace{-\tfrac{\varepsilon^4}{2}\Delta}_{T:=} + \underbrace{H_B^\varepsilon(t)}_{M:=} + \underbrace{\tfrac{1}{2}\|B(t)\,x\|_{\mathbb{R}^d}^2 + \phi(x,t)}_{V:=}. \tag{2.2}$$

The associated Schrödinger equation is given by

$$i\varepsilon^2\partial_t\psi(x,t) = H^\varepsilon\psi(x,t), \quad \psi(x,t_0) = \psi_0(x). \tag{2.3}$$

Let us label the separate equations:

$$i\varepsilon^2 \partial_t \psi(x,t) = T\psi(x,t) \tag{T}$$
$$i\varepsilon^2 \partial_t \psi(x,t) = M\psi(x,t) \tag{M}$$
$$i\varepsilon^2 \partial_t \psi(x,t) = V\psi(x,t) \tag{V}$$

Compared to the standard Schrödinger equation (zero magnetic field), only the term $H_B^\varepsilon(t)$ is new. The time evolution of Equation (M) is simply a rotation of the wave function that depends on the magnetic field $B(t)$. More precisely, consider the ODE

$$\tfrac{\mathrm{d}}{\mathrm{d}t} y(t) = B(t)\, y(t). \tag{B}$$

By [11, Thm X.69] there exists a rotation $R(t,t_0) \in \mathrm{SO}(d)$ such that $y(t) = R(t,t_0)\, y(t_0)$ solves (B) and $R(t_0,t_0) = \mathrm{id}$, that is $R(t,t_0)$ is the flow map associated with (B). Then the wave function

$$\psi(x,t) = \Phi_M(t,t_0)\,\psi_0(x) := \psi_0\left(R^T(t,t_0)\,x\right) \tag{2.4}$$

solves the magnetic equation (M) [6, Lem 2.1] and the corresponding unitary propagator is denoted by $\Phi_M(t,t_0)$. Note that the ODE (B) is independent of the model parameter ε. In our simulations, we approximate the rotation $R(t,t_0)$ by a Magnus expansion. See Section 5 for details. Finally, we observe a crucial structure of our equation

$$H^\varepsilon = \underbrace{T + M}_{\text{commute}} + V.$$

The unitary propagators associated with the Hamiltonians T and M commute [6, Lem 2.3]. The flow map associated with the Hamiltonian $T+M$ thus reads

$$\Phi_{T+M}(t,t_0) = \Phi_T(t,t_0) \circ \Phi_M(t,t_0) = \Phi_M(t,t_0) \circ \Phi_T(t,t_0), \tag{2.5}$$

where

$$\Phi_T(t,t_0) = e^{-i\varepsilon^2(t-t_0)(-\Delta)/2}.$$

3 Hagedorn Wavepackets

We introduce the Hagedorn wavepackets developed in [7] und [8]. However, we use the more modern notation of [4]. Let $q,p \in \mathbb{R}^d$ and $Q,P \in \mathbb{C}^{d\times d}$ with

$$Q^T P - P^T Q = 0, \quad Q^* P - P^* Q = 2i\,\mathrm{id}, \tag{3.1}$$

where Q^* denotes conjugate-transpose and Q^T denotes transpose without complex conjugation. Moreover, we abbreviate $\Pi := (q,p,Q,P)$. Using the vector-valued raising and lowering operators

$$\mathcal{R}^\varepsilon[\Pi] := \frac{i}{\sqrt{2\varepsilon^2}}\left(P^*(x-q) - Q^*\left(-i\varepsilon^2\nabla_x - p\right)\right)$$
$$\mathcal{L}^\varepsilon[\Pi] := -\frac{i}{\sqrt{2\varepsilon^2}}\left(P^T(x-q) - Q^T\left(-i\varepsilon^2\nabla_x - p\right)\right)$$

we define for $k \in \mathbb{N}_0^d$ the Hagedorn wavepackets $\varphi_k^\varepsilon[\Pi]$ recursively by

$$\varphi_0^\varepsilon[\Pi](x) := \left(\pi\varepsilon^2\right)^{-\frac{d}{4}} \sqrt{\det(Q)}\exp\left(\tfrac{i}{2\varepsilon^2}(x-q)^T PQ^{-1}(x-q) + \tfrac{i}{\varepsilon^2}p^T(x-q)\right)$$

and

$$\varphi^{\varepsilon}_{k+e_j}\left[\Pi\right] := \mathcal{R}^{\varepsilon}_j\left[\Pi\right]\varphi^{\varepsilon}_k\left[\Pi\right] \tag{3.2}$$

for all $k \in \mathbb{N}_0^d$ and all $j \in \{1,\ldots,d\}$. We represent the solution of (2.3) in terms of such Hagedorn wavepackets multiplied by a phase factor

$$u\left(x,t\right) = e^{iS(t)/\varepsilon^2}\sum_{k\in\mathcal{K}} c_k\left(t\right)\varphi^{\varepsilon}_k\left[\Pi\left(t\right)\right]\left(x\right), \tag{3.3}$$

where $S\left(t\right)$ is a real-valued function and $\mathcal{K} \subset \mathbb{N}_0$ is a multi-index set. In the numerical simulations of Section 5, we choose [4, Sec.5.4]

$$\mathcal{K} = \left\{ k \in \mathbb{N}_0^d \,|\, \prod_{j=1}^{d}\left(1+k_j\right) \leq K \right\} \tag{3.4}$$

with some truncation constant $K \in \mathbb{N}$. Equation (2.4) asserts that if we can rotate Hagedorn wavepackets, then we can also propagate them according to (M).

Lemma 3.1. *Let $\Pi := (q,p,Q,P)$ satisfy (3.1) and let $R \in \mathrm{SO}\left(d\right)$. Then the rotated parameters*

$$R\Pi := \left(Rq, Rp, RQ, RP\right)$$

still satisfy (3.1) and we have

$$\varphi^{\varepsilon}_k\left[\Pi\right]\left(R^T x\right) = \varphi^{\varepsilon}_k\left[R\Pi\right]\left(x\right) \tag{3.5}$$

for all $\varepsilon > 0$ and all $k \in \mathbb{N}_0^d$.

Proof. We fix $R \in \mathrm{SO}\left(d\right)$ show the formula by induction on $k \in \mathbb{N}_0^d$. For $k = 0$, this is straightforward to verify. Let $\rho\left(R\right)$, be the map that rotates functions by R, i.e.

$$\rho\left(R\right)\varphi\left(x\right) = \varphi\left(R^T x\right)$$

for all $\varphi \in L^2\left(\mathbb{R}^d;\mathbb{C}\right)$. Then a direct computation yields the relation

$$\rho\left(R\right)\mathcal{R}^{\varepsilon}\left[\Pi\right] = \mathcal{R}^{\varepsilon}\left[R\Pi\right]\rho\left(R\right) \tag{3.6}$$

Finally, we fix $j \in \{1,\ldots,d\}$ and compute

$$\begin{aligned}
\rho\left(R\right)\varphi^{\varepsilon}_{k+e_j}\left[\Pi\right] &\overset{(3.2)}{=} \rho\left(R\right)\mathcal{R}^{\varepsilon}_j\varphi^{\varepsilon}_k\left[\Pi\right] \\
&\overset{(3.6)}{=} \mathcal{R}^{\varepsilon}_j\left[R\Pi\right]\rho\left(R\right)\varphi^{\varepsilon}_k\left[\Pi\right] \\
&\overset{(3.5)}{=} \mathcal{R}^{\varepsilon}_j\left[R\Pi\right]\varphi^{\varepsilon}_k\left[R\Pi\right] \\
&\overset{(3.2)}{=} \varphi^{\varepsilon}_{k+e_j}\left[R\Pi\right],
\end{aligned}$$

where we used the induction hypothesis in the third step. This proves (3.5). It is straight forward to check that the rotated parameter satisfy (3.1). □

If we apply this result to $R = R\left(t,t_0\right)$ as in (2.4), we obtain the time evolution of $u\left(x,t\right)$ in (3.3) under (M). The exact time evolution under (M) as been pointed out in [8, Thm 3.4], but without link to rotations (as it covers a more general case).

4 Semiclassical Splitting

We extend the semiclassical splitting developed in [4] and [5] to the Hamiltonian (2.2). We split the Hamiltonian $H = \mathcal{A} + W$ into a local quadratic part

$$\mathcal{A}(t) = T + M + U(x,t)$$

and a remainder $W(x,t)$ at position $q = q(t) \in \mathbb{R}^d$, that is

$$V(x,t) = U(x,t) + W(x,t),$$

where

$$U(x,t) = V(q,t) + \nabla V(q,t) \cdot (x-q) + \tfrac{1}{2}(x-q)^T \nabla^2 V(q,t)(x-q).$$

Here, $\nabla^2 V$ denotes the Hessian of V. The *semiclassial splitting* for a time step $[0,h]$ is

$$\exp\left(-\frac{i}{\varepsilon^2}\cdot\frac{h}{2}\mathcal{A}\left(\tfrac{h}{2}\right)\right)\exp\left(-\frac{i}{\varepsilon^2}hW\left(x,\tfrac{h}{2}\right)\right)\exp\left(-\frac{i}{\varepsilon^2}\cdot\frac{h}{2}\mathcal{A}(0)\right).$$

The exact propagation according to $\mathcal{A}$ in terms of Hagedorn wavepackets requires only propagation of the parameters $\Pi(t) = (q(t), p(t), Q(t), P(t))$ and $S(t)$ of the function $u(x,t)$ defined in (3.3). The coefficients $(c_k)_{k\in\mathcal{K}}$ remain constant. More precisely, we have

$$i\varepsilon^2 \partial_t u(x,t) = \mathcal{A}(t)\, u(x,t)$$

if the parameters solve the ODE

$$\begin{aligned}
\dot{q}(t) &= p(t) + B(t)\, q(t) \\
\dot{Q}(t) &= P(t) + B(t)\, Q(t) \\
\dot{S}(t) &= \tfrac{1}{2}\|p(t)\|^2_{\mathbb{R}^d} - U(q(t)) \\
\dot{p}(t) &= -\nabla U(q(t)) + B(t)\, p(t) \\
\dot{P}(t) &= -\nabla^2 U(q(t))\, Q(t) + B(t)\, P(t),
\end{aligned} \tag{4.1}$$

where $B(t) \in \mathbb{R}^{d\times d}$ denotes the skew symmetric magnetic field matrix. We split this ODE into three parts that correspond to Equations (T), (M) and (V) (the latter with quadratic potential). These separate ODEs can then be solved using the basic time-propagation properties of Hagedorn wavepackets due to [8, Thm 3.4] and [4]. We only summarize the propagation steps we use subsequently:

(i) If $\Pi(t)$ satisfies

$$\begin{aligned}
q(t) &= q(t_0) + (t-t_0)\, p(t_0) \\
Q(t) &= Q(t_0) + (t-t_0)\, P(t_0) \\
S(t) &= S(t_0) + \tfrac{1}{2}(t-t_0)\,\|p(t_0)\|^2_{\mathbb{R}^d}.
\end{aligned}$$

and all other parameters and the coefficients remain constant, then $u(x,t)$ solves the kinetic equation (T), i.e.

$$i\varepsilon^2 \partial_t u(x,t) = T u(x,t).$$

For details, see [4, Prop 2.1].

(ii) Let $R(t,t_0)$ be the flow map associated with the ODE

$$\tfrac{\mathrm{d}}{\mathrm{d}t}y(t) = B(t)\,y(t). \tag{B}$$

If $\Pi(t)$ satisfies

$$\begin{aligned} q(t) &= R(t,t_0)\,q(t_0) \\ p(t) &= R(t,t_0)\,p(t_0) \\ Q(t) &= R(t,t_0)\,Q(t_0) \\ P(t) &= R(t,t_0)\,P(t_0) \end{aligned}$$

and $S(t)$ and the coefficients remain constant, then $u(x,t)$ solves the magnetic equation (M), i.e.

$$i\varepsilon^2\partial_t u(x,t) = M(t)\,u(x,t).$$

See Lemma 3.1 and Equation (2.4) for details.

(iii) Let $U(x,t)$ be a quadratic potential and denote its Hessian by $\nabla^2 U$. If $\Pi(t)$ satisfies

$$\begin{aligned} p(t) &= p(t_0) - (t-t_0)\,\nabla U(q(t_0),t_0) \\ P(t) &= P(t_0) - (t-t_0)\,\nabla^2 U(q(t_0),t_0)\cdot Q(t_0) \\ S(t) &= S(t_0) - (t-t_0)\,U(q(t_0),t_0) \end{aligned}$$

and all other parameters and the coefficients remain constant, then $u(x,t)$ solves the potential equation (V) for $V(x,t) = U(x,t_0)$, i.e.

$$i\varepsilon^2\partial_t u(x,t) = U(x,t_0)\,u(x,t).$$

For details, see [4, Prop 2.2].

(iv) This applies in particular to the quadratic potential $\frac{1}{2}\|B(t)\,x\|^2_{\mathbb{R}^d}$ in (2.2). We just have to substitute

$$U(x,t) = \tfrac{1}{2}\|B(t)\,x\|^2_{\mathbb{R}^d}, \quad \nabla U(x,t) = -B^2(t)\,x, \quad \nabla^2 U(x,t) \equiv -B^2(t).$$

(v) The propagators in (i) and (ii) commute and thus their concatenation yields the exact propagation for the Hamiltonian $T + M(t)$. As a consequence, we can solve the system ODEs (4.1) with only one effective splitting (namely between $T + M(t)$ and $U(x,t_0)$), like in the zero magnetic field case (see [4]). This is just the parameter version of Equation (2.5).

Note that all these propagation steps leave the coefficients $(c_k)_{k\in\mathcal{K}}$ unaltered and only change the parameters $\Pi(t)$ and $S(t)$. Moreover, by Item (v) the only additional effort compared to the zero magnetic field case is to solve the low-dimensional ODE (M). For this *inner splitting*, we use the same splitting method of order 8 as in [2] to produce comparable results.
It remains to solve the equation for the remainder with time frozen at t_0, that is

$$i\varepsilon^2\partial_t u(x,t) = W(x,t_0)\,u(x,t).$$

This is done exactly as in the zero magnetic field case, see [4, Sec.2.5]. The Galerkin matrix of the remainder w.r.t. the Hagedorn wavepacket basis

$$F_{j,k}[\Pi(t_0)] = \int_{\mathbb{R}^d} \overline{\varphi_j^\varepsilon[\Pi(t_0)](x)}\,W(x,t_0)\,\varphi_k^\varepsilon[\Pi(t_0)](x)\,\mathrm{d}x, \quad j,k\in\mathcal{K},$$

yields an ODE for the coefficients $(c_k(t))_{k\in\mathcal{K}}$, namely

$$i\varepsilon^2\dot{c}(t) = F[\Pi(t_0)]\,c(t).$$

A splitting step w.r.t. W therefore reads

$$c(t) = \exp\left(-\frac{i}{\varepsilon^2}(t-t_0)\,F[\Pi(t_0)]\right)c(t_0)$$

and the parameters $\Pi(t_0)$ and $S(t_0)$ stay unaltered. As in [2], we point out the following: The remainder W perturbs the solution w.r.t. A by order $\mathcal{O}(\varepsilon^3)$ as $\varepsilon \to 0$ (see [5, Lem. 3]). This will be used in the next section.

5 Splitting Schemes

We follow the discussion of splitting schemes in [2, Sec. 3] and consider a differential equation of the form

$$\dot{x} = \mathcal{A}x + \mathcal{B}x, \quad x(0) = x_0 \in \mathbb{R}^d \tag{5.1}$$

with the (time-independent) vector fields

$$\mathcal{A} = \sum_{j=1}^{d} \mathcal{A}^j(x)\,\partial_j \quad \text{and} \quad \mathcal{B} = \sum_{j=1}^{d} \mathcal{B}^j(x)\,\partial_j.$$

We denote the corresponding flow maps with time step $h \in \mathbb{R}$ by

$$\varphi_h^{\mathcal{A}} = \exp(h\mathcal{A}) \quad \text{and} \quad \varphi_h^{\mathcal{B}} = \exp(h\mathcal{B}).$$

For splitting coefficients $a, b \in \mathbb{R}^s$, we denote the corresponding splitting scheme by

$$\varphi_h^{\mathcal{A}} \overset{(a,b)}{\circ} \varphi_h^{\mathcal{B}} = \varphi_{a_1 h}^{\mathcal{A}} \circ \varphi_{b_1 h}^{\mathcal{B}} \circ \cdots \circ \varphi_{a_s h}^{\mathcal{A}} \circ \varphi_{b_s h}^{\mathcal{B}}. \tag{5.2}$$

Note that the action of the exponentials is in reverse order that they are written. So in terms of the flow maps $\Phi_{\mathcal{A}}$ and $\Phi_{\mathcal{B}}$ of $\mathcal{A}$ and $\mathcal{B}$, the splitting method (5.2) reads

$$\Phi_{\mathcal{B}}(b_s h) \circ \Phi_{\mathcal{A}}(a_s h) \circ \cdots \circ \Phi_{\mathcal{B}}(b_1 h) \circ \Phi_{\mathcal{A}}(a_1 h).$$

For a motivation of this notation, we refer to [1, Sec. A.1].

5.1 Splittings for Perturbed Systems

A consistent splitting scheme takes the form

$$\varphi_h^{\mathcal{A}} \overset{(a,b)}{\circ} \varphi_h^{\mathcal{B}} = \exp\left(h\left(\mathcal{A} + \mathcal{B} + E(h)\right)\right),$$

with remainder

$$\begin{aligned} E(h) = {} & h\nu_{ab}[\mathcal{A},\mathcal{B}] + h^2\nu_{aab}[\mathcal{A},[\mathcal{A},\mathcal{B}]] + h^2\nu_{bab}[\mathcal{B},[\mathcal{A},\mathcal{B}]] \\ & + h^3\nu_{aaab}[\mathcal{A},[\mathcal{A},[\mathcal{A},\mathcal{B}]]] + h^3\nu_{baab}[\mathcal{B},[\mathcal{A},[\mathcal{A},\mathcal{B}]]] \\ & + h^3\nu_{bbab}[\mathcal{B},[\mathcal{B},[\mathcal{A},\mathcal{B}]]] + \mathcal{O}\left(h^4\right) \end{aligned}$$

Suppose now that the vector field $\mathcal{B}$ is merely a perturbation of $\mathcal{A}$, say $\mathcal{B} = \varepsilon\mathcal{B}_0$ for some small $\varepsilon > 0$ and a vector field $\mathcal{B}_0$ of same scale as $\mathcal{A}$. Then the remainder becomes

$$\begin{aligned} E(h,\varepsilon) = {} & h\varepsilon\nu_{ab}[\mathcal{A},\mathcal{B}_0] + h^2\varepsilon\nu_{aab}[\mathcal{A},[\mathcal{A},\mathcal{B}_0]] + h^2\varepsilon^2\nu_{bab}[\mathcal{B}_0,[\mathcal{A},\mathcal{B}_0]] \\ & + h^3\varepsilon\nu_{aaab}[\mathcal{A},[\mathcal{A},[\mathcal{A},\mathcal{B}_0]]] + h^3\varepsilon^2\nu_{baab}[\mathcal{B}_0,[\mathcal{A},[\mathcal{A},\mathcal{B}_0]]] \\ & + h^3\varepsilon^3\nu_{bbab}[\mathcal{B}_0,[\mathcal{B}_0,[\mathcal{A},\mathcal{B}_0]]] + \mathcal{O}\left(h^4\right). \end{aligned}$$

In this case, we say the method (5.2) is or generalized order $(r_1, r_2, \ldots, r_m)$, where $r_1 \geq r_2 \geq \cdots \geq r_m$, if the remainder satisfies

$$E(h,\varepsilon) = \mathcal{O}\left(\varepsilon h^{r_1} + \varepsilon^2 h^{r_2} + \cdots + \varepsilon^m h^{r_m}\right).$$

The choice $a = \left(\frac{1}{2}, \frac{1}{2}\right)$ and $b = (1, 0)$ leads to the well-known *Strang splitting*, which is of order 2. A symmetric, perturbation aware splitting is for example the method of generalized order $(4, 2)$

$$\Psi_{(4,2)}(h) = e^{a_1 h\mathcal{A}} e^{b_1 h\mathcal{B}} e^{a_2 h\mathcal{A}} e^{b_1 h\mathcal{B}} e^{a_1 h\mathcal{A}},$$

with $a_1 = \frac{1}{6}\left(3 - \sqrt{3}\right), a_2 = 1 - 2a_1, b_1 = \frac{1}{2}$, or the method of generalized order $(8, 4)$

$$\Psi_{(8,4)}(h) = e^{a_1 h\mathcal{A}} e^{b_1 h\mathcal{B}} e^{a_2 h\mathcal{A}} e^{b_2 h\mathcal{B}} e^{a_3 h\mathcal{A}} e^{b_3 h\mathcal{B}} e^{a_3 h\mathcal{A}} e^{b_2 h\mathcal{B}} e^{a_2 h\mathcal{A}} e^{b_1 h\mathcal{B}} e^{a_1 h\mathcal{A}},$$

with coefficients given in Table 1.

$a_1 = 0.0753469602698929$	$a_2 = 0.5179168546882568$	$a_3 = \frac{1}{2} - (a_1 + a_2)$
$b_1 = 0.1902259393736766$	$b_2 = 0.8465240704435263$	$b_3 = 1 - 2(b_1 + b_2)$

Table 1: Coefficients for the $(8, 4)$ symmetric splitting.

5.2 Processed Methods for Perturbed Systems

In this section, we improve our splitting schemes using a *pre-processor*, i.e. a map $\pi_h : \mathbb{R}^d \to \mathbb{R}^d$, such that the method

$$\widetilde{\Psi}(h) = \pi_h^{-1} \circ \Psi(h) \circ \pi_h,$$

is more accurate than $\Psi(h)$. The n-fold concatenation $\widetilde{\Psi}^n(h)$ of the processed method then satisfies $\widetilde{\Psi}^n(h) = \pi_h^{-1} \circ \Psi^n(h) \circ \pi_h$. Thus it is as expensive as the n-fold concatenation $\Psi^n(h)$ of the non-processed method and still more accurate. In our simulations, we will examine the processed method of generalized order $(7, 6, 4)$ given by

$$\widetilde{\Psi}_{(7,6,4)}(h) = \left(e^{-h\mathcal{A}} \overset{(z,y)}{\circ} e^{-h\mathcal{B}}\right) \circ \left(e^{h\mathcal{A}} \overset{(a,b)}{\circ} e^{h\mathcal{B}}\right) \circ \left(e^{h\mathcal{B}} \overset{(y,z)}{\circ} e^{h\mathcal{A}}\right), \tag{5.3}$$

with coefficients given in Table 2.

$a_1 = 0.5600879810924619$	$a_2 = \frac{1}{2} - a_1$	
$b_1 = 1.5171479707207228$	$b_2 = 1 - 2b_1$	
$z_1 = -0.3346222298730800$	$z_2 = 1.0975679907321640$	$z_3 = -1.0380887460967830$
$z_4 = 0.6234776317921379$	$z_5 = -1.1027532063031910$	$z_6 = -0.0141183222088869$
$y_1 = -1.6218101180868010$	$y_2 = 0.0061709468110142$	$y_3 = 0.8348493592472594$
$y_4 = -0.0511253369989315$	$y_5 = 0.5633782670698199$	$y_6 = -0.5$

Table 2: Coefficients for the $(7, 6, 4)$ processed splitting.

5.3 Processed Methods With Modified Potentials for Perturbed Systems

We split our Hamiltonian of interest (2.2) into a sum of the local quadratic part

$$\mathcal{A}(t) = -\tfrac{i}{\varepsilon^2}\left(T + M(t) + U(x,t)\right)$$

and the non-quadratic remainder

$$\mathcal{B}(t) = -\tfrac{i}{\varepsilon^2} W(x,t),$$

where for every fixed $t \in \mathbb{R}$, we have $V(x,t) = U(x,t) + W(x,t)$ with $U(x,t)$ the local quadratic Taylor expansion of $V(x,t)$ at position $q(t) \in \mathbb{R}^d$. As mentioned above, $W(\cdot,t)$ perturbs the solution (w.r.t. $\mathcal{A}(t)$) by $\mathcal{O}(\varepsilon^3)$. Hence the theory of the previous sections applies, that is we interpret $\mathcal{B}(t)$ as a perturbation of of order $\mathcal{O}(\varepsilon)$. Moreover, we have

$$\left[-iH_{\mathcal{B}}(t), -\tfrac{i}{\varepsilon^2} W(x,t)\right] = -\left(H_B(t)\, W(x,t)\right)$$

and hence

$$\left[-\tfrac{i}{\varepsilon^2} W(x,t), \left[-iH_B(t), -\tfrac{i}{\varepsilon^2} W(x,t)\right]\right] = 0.$$

On the other hand, we have [2, Sec. 3.4]

$$\left[-\tfrac{i}{\varepsilon^2} W(x,t), \left[T + U(x,t), -\tfrac{i}{\varepsilon^2} W(x,t)\right]\right] = -\frac{i}{\varepsilon^2}\left(-\nabla_x W(x,t) \cdot \nabla_x W(x,t)\right).$$

The last two equations together yield

$$\left[\mathcal{B}(t), \left[\mathcal{A}(t), \mathcal{B}(t)\right]\right] = -\frac{i}{\varepsilon^2}\left(-\nabla_x W(x,t) \cdot \nabla_x W(x,t)\right).$$

This modified potential is exactly the same as in the zero magnetic field case in [2]. We can thus use the same modified propagator as proposed in [2, Sec. 3.5], namely

$$\varphi_{h,h/24} = \exp\left(h\mathcal{B}(t) + \frac{h^3}{24}\left[\mathcal{B}(t), \left[\mathcal{A}(t), \mathcal{B}(t)\right]\right]\right).$$

Here, we think of the time to be frozen at t. It can be evaluated at a similar computational cost as $e^{h\mathcal{B}}$, as explained in [2, Sec. 3.4]. Analogous to [2, Eq. (19)], we obtain a method of generalized order $(6, 4)$ by

$$\Psi_{(6,4)}(h) = \left(e^{-h\mathcal{B}} \overset{(y,z)}{\circ} e^{-h\mathcal{A}}\right) \circ \left(e^{\frac{h}{2}\mathcal{A}} \circ \varphi_{h,h/24} \circ e^{\frac{h}{2}\mathcal{A}}\right) \circ \left(e^{h\mathcal{A}} \overset{(z,y)}{\circ} e^{h\mathcal{B}}\right), \tag{5.4}$$

with processing coefficients given in Table 3. This is basically a processed Strang splitting. Consequently, this method is of similar computational cost as the semiclassical splitting, but provides highly improved accuracy.

$y_1 = -0.1659120515409654$	$y_2 = -0.1237659000825160$	$y_3 = 0.0250397323738759$
$y_4 = 0.2269372219010943$		
$z_1 = -0.9125829692505096$	$z_2 = -0.3605243318856133$	$z_3 = 0.7354063037876117$
$z_4 = 0.5$		

Table 3: Coefficients for the $(6, 4)$ processed splitting.

5.4 Splitting Methods for Non-Autonomous Systems

We apply the same autonomization as proposed in [2, Sec. 3]. Our problem can be written as a perturbed, non-autonomous system

$$\dot{\psi} = \mathcal{A}(t)\,\psi + \mathcal{B}(t)\,\psi, \quad \psi(t_0) = \psi_0 \tag{5.5}$$

with

$$-i\mathcal{A}(t) = T + M(t) + U(x,t) \quad \text{and} \quad -i\mathcal{B}(t) = \tfrac{1}{\varepsilon^2} W(x,t),$$

where $\mathcal{B}(t)$ is a perturbation of $\mathcal{A}(t)$ for small model parameters $\varepsilon > 0$. In order to apply the theory discussed so far, we consider the equivalent autonomous equation for $\psi = \psi(t)$ and $s = s(t)$ given by

$$\partial_t \begin{pmatrix} \psi \\ s \end{pmatrix} = \begin{pmatrix} -i\frac{1}{\varepsilon^2}\mathcal{A}(s)\,\psi \\ 1 \end{pmatrix} + \begin{pmatrix} -i\frac{1}{\varepsilon^2}\mathcal{B}(s)\,\psi \\ 0 \end{pmatrix}, \quad \psi(t_0) = \psi_0, \quad s(t_0) = t_0.$$

Furthermore, we introduce the vector fields

$$\tilde{\mathcal{A}} = \mathcal{A}(s)\,\tfrac{\delta}{\delta\psi} + 1 \cdot \tfrac{\delta}{\delta s} \quad \text{and} \quad \tilde{\mathcal{B}} = \mathcal{B}(s)\,\tfrac{\delta}{\delta\psi}.$$

With $u = (\psi, s)$, we can rewrite the above equation as

$$\dot{u} = \tilde{\mathcal{A}}(u) + \tilde{\mathcal{B}}(u).$$

A short computation yields

$$\left[\tilde{\mathcal{B}}, \left[\tilde{\mathcal{A}}, \tilde{\mathcal{B}}\right]\right] = -\tfrac{i}{\varepsilon^2}\nabla_x W(x,s) \cdot \nabla_x W(x,s)\tfrac{\delta}{\delta\psi}.$$

Thus we are in the situation of the previous subsections. To summarize, we need to solve the autonomous equation (W frozen at time t_0)

$$\dot{\psi} = -\tfrac{i}{\varepsilon^2} W(x,t_0)\,\psi, \quad \psi(t_0) = \psi_0,$$

or in case of (5.4) the autonomous equation

$$\dot{\psi} = -\frac{i}{\varepsilon^2}\left(W(x,t_0) - \tfrac{h^2}{24}\nabla_x W(x,t_0) \cdot \nabla_x W(x,t_0)\right), \quad \psi(t_0) = \psi_0.$$

Furthermore, we need to solve the non-autonomous equation

$$\dot{\psi} = \mathcal{A}(t)\,\psi, \quad \psi(t_0) = \psi_0 \tag{5.6}$$

either exact or to high precision. The momentum part $T + M(t)$ needs to be split into

$$\partial_t \begin{pmatrix} \psi \\ s \end{pmatrix} = \begin{pmatrix} -i\frac{1}{\varepsilon^2} T\psi \\ 0 \end{pmatrix} \quad \text{and} \quad \partial_t \begin{pmatrix} \psi \\ s \end{pmatrix} = \begin{pmatrix} -i\frac{1}{\varepsilon^2} M(s)\,\psi \\ 1 \end{pmatrix}. \tag{5.7}$$

It is crucial to perform the evolution of $s(t)$ together with $M(s)$, so that the exact flow maps of the two equations commute. Their concatenation then yields the exact flow map of the momentum equation as in (5.7). Finally, it remains to solve Equation (B) exactly or to very high accuracy.

6 Numerical Simulation

In the subsequent simulations we thus use a truncated version of (3.3). The flow map $R(t, t_0) \in \mathrm{SO}(d)$ of (B), which is needed for Φ_M, will be approximated by the fourth-order commutator-free Magnus expansion in [3]. See [6, Example 2.1] for a detailed explanation in our case. To verify our method, we plot the energies along the approximate solution $u(t)$ for unit charge and unit mass:

$$\begin{aligned}
E^{\varepsilon}_{\mathrm{kin}}(t) &:= \langle u(t), -\tfrac{\varepsilon^4}{2}\Delta u(t)\rangle_{L^2} && \text{(kinetic energy)}\\
E^{\varepsilon}_{\mathrm{mag}}(t) &:= \langle u(t), \left(H^{\varepsilon}_B(t) + \tfrac{1}{2}\|B(t)\,x\|^2_{\mathbb{R}^d}\right) u(t)\rangle_{L^2} && \text{(magetic energy)}\\
E_{\mathrm{pot}}(t) &:= \langle u(t), \phi(x)\, u(t)\rangle_{L^2} && \text{(potential energy)}\\
E^{\varepsilon}_{\mathrm{tot}}(t) &:= E^{\varepsilon}_{\mathrm{kin}}(t) + E^{\varepsilon}_{\mathrm{mag}}(t) + E_{\mathrm{pot}}(t). && \text{(total energy)}
\end{aligned}$$

The inner products for $E^{\varepsilon}_{\mathrm{kin}}$ and $E^{\varepsilon}_{\mathrm{mag}}$ can be computed only in terms of the coefficients For a good approximate solution, we expect approximate conservation of total energy.

6.1 Penning Trap (single particle)

We consider a particle of unit mass ($m = 1$) and unit charge ($e = 1$) in $d = 3$ dimensions in a Penning trap. We use the Hamiltonian proposed in [9], namely the time-independent Hamiltonian

$$H^{x}_{\mathrm{trap}} := -\tfrac{\varepsilon^4}{2}\Delta + H^{\varepsilon}_B + \tfrac{e^2}{2}\|Bx\|^2_{\mathbb{R}^3} + \phi_{\mathrm{trap}}(x)$$

with $\varepsilon = 0.01$ and electric potential

$$\phi_{\mathrm{trap}}(x) = \frac{1}{2}\left(x_3^2 - \frac{x_1^2 + x_2^2}{2}\right) \tag{6.1}$$

and a magnetic field enclosing the angle $\Theta = 0.4$ with the z-axis

$$\vec{B} = 2\begin{pmatrix}\sin(\Theta)\\ 0\\ \cos(\Theta)\end{pmatrix}.$$

The corresponding vector potential is $\vec{A} = \frac{1}{2}\left(\vec{B}\times\vec{x}\right)$, which is represented by the time-independent skew-symmetric matrix

$$B = \begin{pmatrix} 0 & \cos(\Theta) & 0\\ -\cos(\Theta) & 0 & \sin(\Theta)\\ 0 & -\sin(\Theta) & 0\end{pmatrix}. \tag{6.2}$$

The initial data is given by $u(x,0) = \varphi^{\varepsilon}_0[\Pi(0)](x)$, where $\Pi(0) = (q,p,Q,P)$ and

$$q = (1,0,1), \quad p = (0,-1,0), \quad Q = \mathrm{id}, \quad P = i\cdot\mathrm{id}. \tag{6.3}$$

Since the potential is quadratic, we only need to propagate the parameters $\Pi(t)$ and $S(t)$ in (3.3). Therefore, we choose $\mathcal{K} = \{(0,0,0)\}$. The energies along the approximate solution by semiclassical splitting are shown in Figure 1.

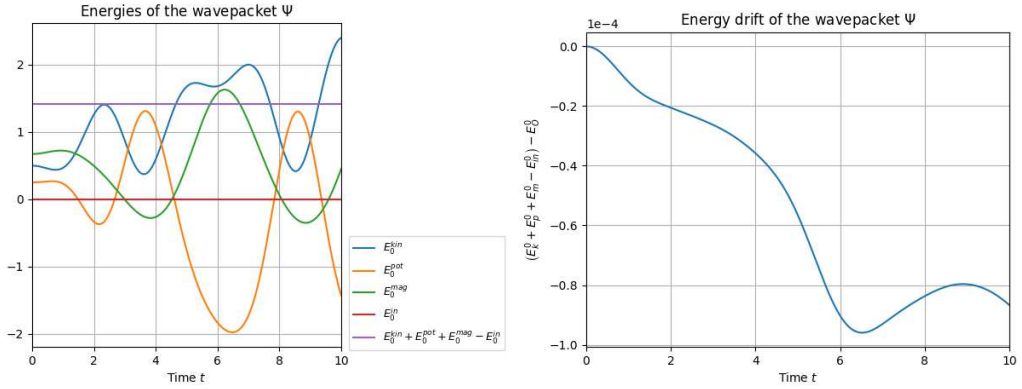

Figure 1: Single particle in a Penning trap: Total energy along the computed solution is conserved.

6.2 Penning Trap (two particles)

We consider two charged particles of unit mass and charge in the same Penning trap as before. We write $x = \left(x^{(1)}, x^{(2)}\right) \in \mathbb{R}^3 \times \mathbb{R}^3$ for the coordinates of the particles. The repulsion between the particles is modeled by a Mie(4,2) potential [10], [6, Sec.3.5]

$$\phi_{\text{rep}}(x) = 32 \cdot \left(\frac{3^4}{\|x^{(1)} - x^{(2)}\|_{\mathbb{R}^3}^4} - \frac{3^2}{\|x^{(1)} - x^{(2)}\|_{\mathbb{R}^3}^2} \right) + 8.$$

The Hamiltonian on $L^2(\mathbb{R}^6; \mathbb{C})$ is then given by $H_{\text{trap}}^{x^{(1)}} + H_{\text{trap}}^{x^{(2)}} + \phi_{\text{rep}}(x)$ or equivalently

$$-\tfrac{\varepsilon^4}{2}\Delta + H_B^\varepsilon + \tfrac{1}{2}\|Bx\|_{\mathbb{R}^6}^2 + \phi(x),$$

where

$$\phi(x) = \phi_{\text{trap}}\left(x^{(1)}\right) + \phi_{\text{trap}}\left(x^{(2)}\right) + \phi_{\text{rep}}(x) \quad \text{and} \quad B = \begin{pmatrix} B^{(1)} & 0 \\ 0 & B^{(2)} \end{pmatrix},$$

where $B^{(1)} = B^{(2)}$ are two copies of the matrix in (6.2). The initial data is chosen to be $u(x,0) = \varphi_0^\varepsilon[\Pi(0)](x)$, where $\Pi(0) = (q,p,Q,P)$ and

$$q = (\underbrace{2,0,2}_{q^{(1)}}, \underbrace{0,-3,0}_{q^{(2)}}), \quad p = (\underbrace{0,-1,0}_{p^{(1)}}, \underbrace{0,0,1}_{p^{(2)}}), \quad Q = \text{id}, \quad P = i \cdot \text{id}.$$

Since the repulsion $\phi_{\text{rep}}(x)$ is non-quadratic, we have to propagate also the coefficients $(c_k(t))_{k\in\mathcal{K}}$ in (3.3). We use the fixed index set $\mathcal{K}$ as in (3.4) for $d = K = 6$. The energies along the approximate solution are plotted in Figure 2.

6.3 Convergence of the Different Splittings

We analyse the convergence in time and for different model parameters $\varepsilon > 0$. To this end, we use a single particle in $d = 3$ dimensions, subject to a Morse potential

$$\phi_{\text{Morse}}(x) = 8 \cdot (\exp(-2 \cdot 0.3 \cdot (\|x\|_{\mathbb{R}^3} - 4)) - 2 \cdot \exp(-0.3 \cdot (\|x\|_{\mathbb{R}^3} - 4))) + 8.$$

the magnetic field is given by

$$B(t) = \begin{pmatrix} 0 & \cos(\pi t) & 0 \\ -\cos(\pi t) & 0 & \sin(\pi t) \\ 0 & \sin(\pi t) & 0 \end{pmatrix}.$$

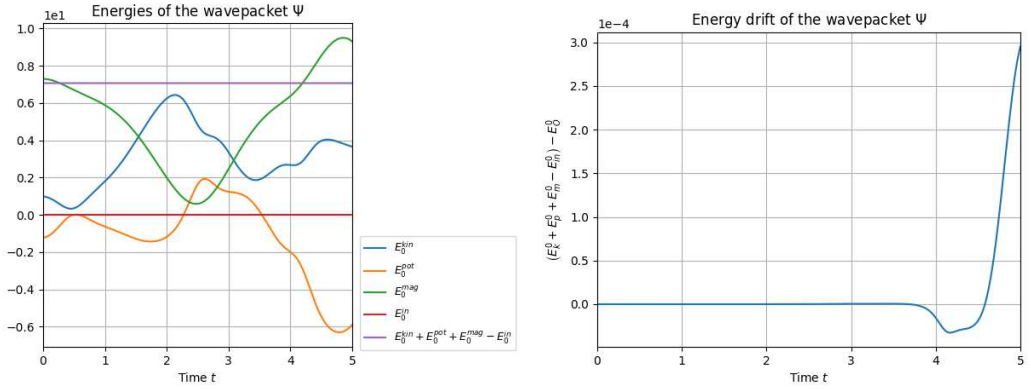

Figure 2: Two particles in the Penning trap: Total energy along the computed solution is conserved.

We solve the Schrödinger equation on the time interval $[0, 2]$ with initial data $u(x, 0) = \varphi_0^\varepsilon [\Pi(0)](x)$, where $\Pi(0) = (q, p, Q, P)$ is the same as in (6.3). The index set $\mathcal{K}$ in (3.4) is truncated by $K = 32$ for both the approximate and the reference solution. The latter was computed with the modified potential splitting (5.4) of time steps of size $h = 2^{-6}$. The plots below show the L^2-difference to reference solution at final time $T = 2$. The L^2-norm was computed by a scaled and very accurate Gauss-Hermite quadrature as described in [4, Sec.4.1]. The results are qualitatively the same as for the standard Schrödinger equation in [5, Fig.5]. In particular, the methods improve for small values of ε.

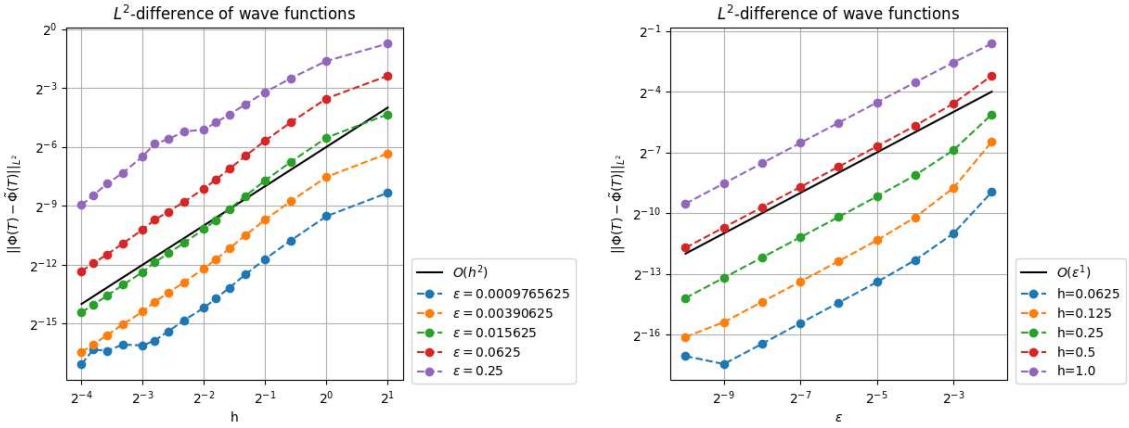

Figure 3: Semiclassical splitting of order 2 as described in Section 4.

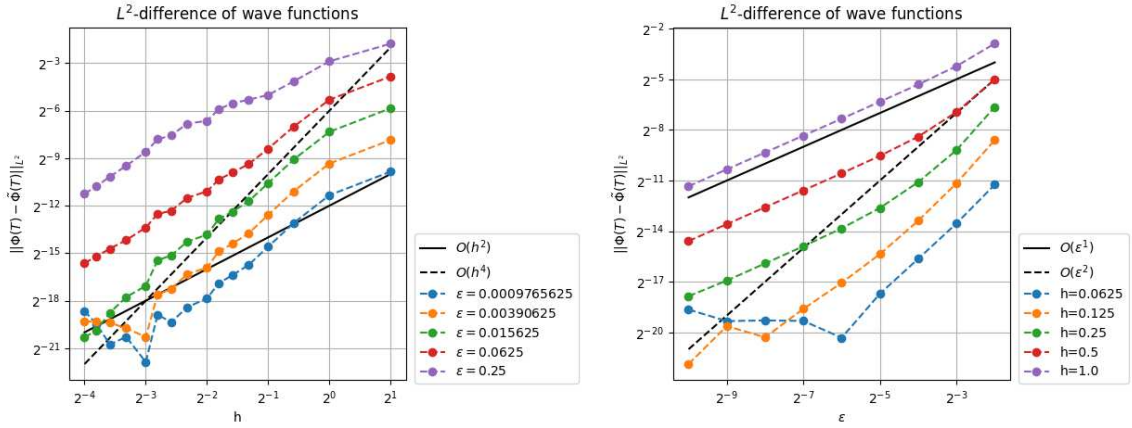

Figure 4: Perturbation-aware splitting of generalized order $(4, 2)$ as described in Section 5.1.

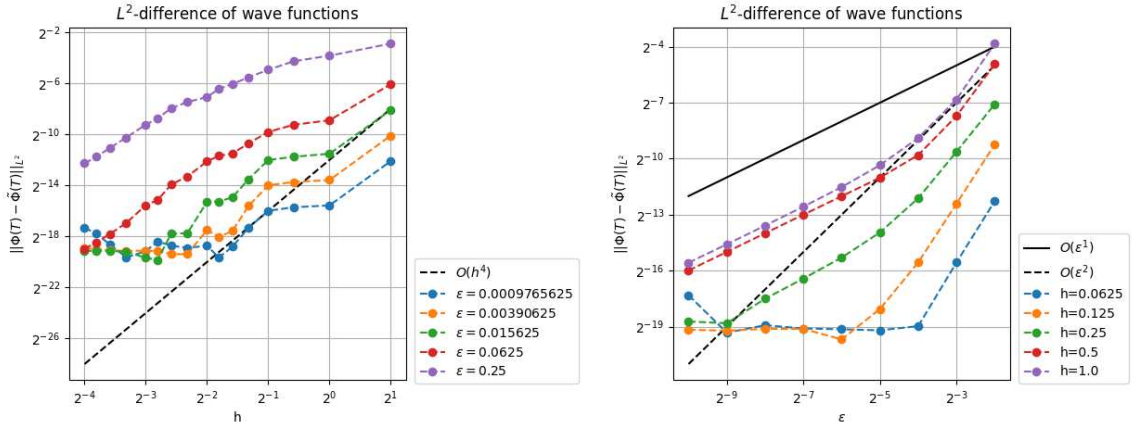

Figure 5: Perturbation-aware splitting of generalized order $(8, 4)$ as described in Section 5.1. The splitting coefficients are given in Table 1.

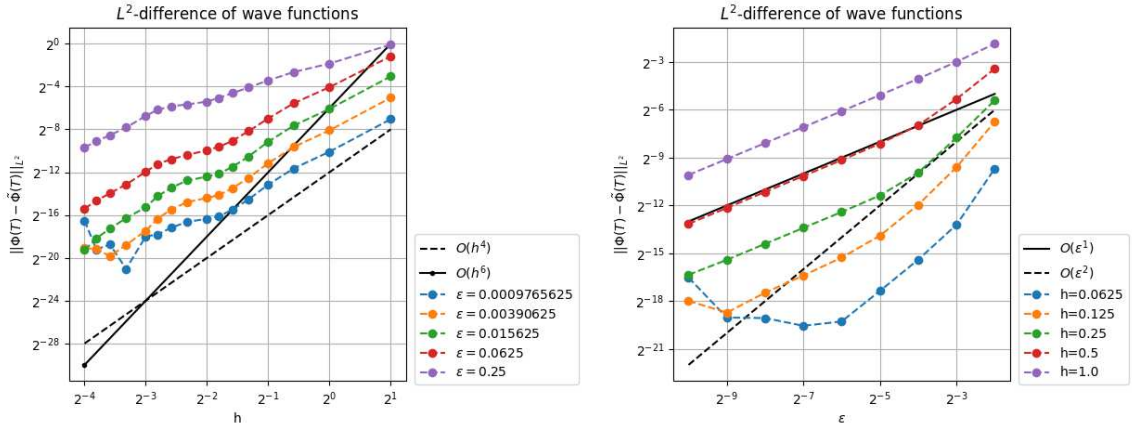

Figure 6: Perturbation-aware processed splitting of generalized order $(7, 6, 4)$ as described in Section 5.2. The splitting coefficients are given in Table 2.

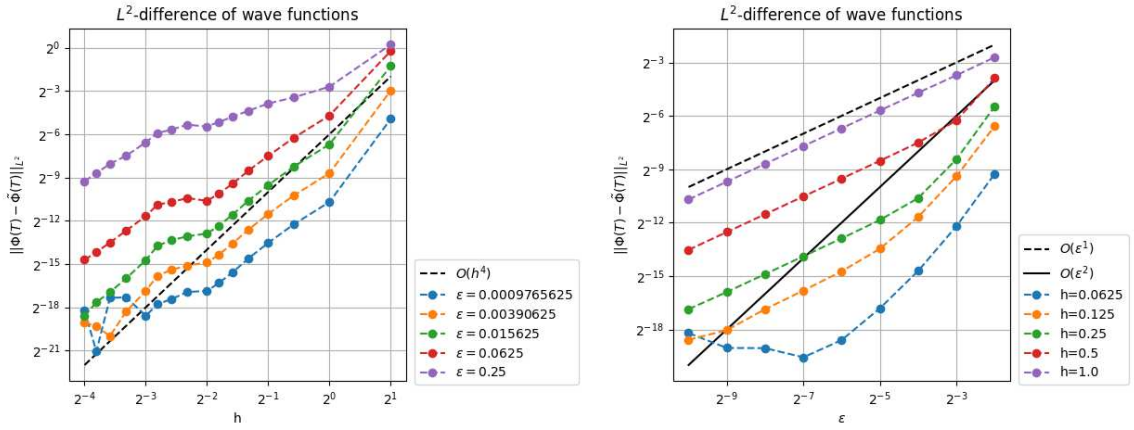

Figure 7: Perturbation-aware processed splitting with modified potential of generalized order $(6, 4)$ as described in Section 5.3. The splitting coefficients are given in Table 3.

References

[1] S. Blanes and F. Casas. *A Concise Introduction to Geometric Numerical Integration*. Chapman & Hall/CRC Monographs and Research Notes in Mathematics. CRC Press, 2017.

[2] Sergio Blanes and Vasile Gradinaru. High order efficient splittings for the semiclassical time–dependent schrödinger equation. *Journal of Computational Physics*, 405:109157, 2020.

[3] Sergio Blanes and Per Christian Moan. Fourth- and sixth-order commutator-free Magnus integrators for linear and non-linear dynamical systems. *Applied Numerical Mathematics*, 56(12):1519 – 1537, 2006.

[4] Erwan Faou, Vasile Gradinaru, and Christian Lubich. Computing semiclassical quantum dynamics with Hagedorn wavepackets. *SIAM J. Scientific Computing*, 31:3027–3041, 01 2009.

[5] Vasile Gradinaru and George A. Hagedorn. Convergence of a semiclassical wavepacket based time-splitting for the schrödinger equation. *Numerische Mathematik*, 126(1):53–73, Jan 2014.

[6] Vasile Gradinaru and Oliver Rietmann. A high-order integrator for the schrödinger equation with time-dependent, homogeneous magnetic field. Technical Report 2018-47, Seminar for Applied Mathematics, ETH Zürich, Switzerland, 2018.

[7] G. A. Hagedorn. Semiclassical quantum mechanics. i. the $\hbar \to 0$ limit for coherent states. *Comm. Math. Phys.*, 1(1):77–93, 1980.

[8] George Hagedorn. Raising and lowering operators for semiclassical wave packets. *Annals of Physics*, 269(1):77 – 104, 1998.

[9] Shreyans Jain, Joseba Alonso, Matt Grau, and Jonathan P. Home. Quantum simulation with ions in micro-fabricated Penning traps. *arXiv e-prints*, page arXiv:1812.06755, Dec 2018.

[10] Gustav Mie. Zur kinetischen theorie der einatomigen körper. *Annalen der Physik*, 316(8):657–697, 1903.

[11] Barry Simon and Michael Reed. *Fourier analysis, self-adjointness*, volume 2 of *Methods of modern mathematical physics*. Academic Press, Boston, 1975.

[12] Zhennan Zhou. Numerical approximation of the Schrödinger equation with the electromagnetic field by the Hagedorn wave packets. *Journal of Computational Physics*, 272:386–407, 09 2014.